IBRO Neuroscience Reports 13 (2022) 274–283

Contents lists available at ScienceDirect

IBRO Neuroscience Reports

journal homepage: www.sciencedirect.com/journal/IBRO-Neuroscience-Reports

Research Paper

Differences in the neural networks of thermal sensation with and without evaluation process

Kei Nagashima [a,*], Hiroki Nakata [b], Tokiko Harada [c,d], Issei Kato [a,e], Norihiro Sadato [c]

[a] Body Temperature and Fluid Laboratory, Faculty of Human Sciences, Waseda University, Mikajima 2-579-15, Tokorozawa, Saitama 359-1192, Japan
[b] Faculty of Engineering, Nara Women's University, Nara Women's University, Kitauoya-Higashimachi, Nara, Nara 630-8506, Japan
[c] Department of System Neuroscience, National Institute for Physiological Sciences, Myodaiji, Okazaki, Aichi 444-8585, Japan
[d] Graduate School of Informatics, Nagoya University, Furo-cho, Chikusa-ku, Nagoya, Aichi 464-8601, Japan
[e] Graduate School of Human Sciences, Waseda University, Mikajima 2-579-15, Tokorozawa, Saitama 359-1192, Japan

A B S T R A C T

Several neuroimaging studies have analyzed the neural networks involved in thermal sensation. In some of these studies, participants were instructed to evaluate and report the thermal sensation using a point scale, visual analog scale, or other psychophysical rating tool while the imaging data were obtained. Therefore, the imaging data may reflect signals involved in the processes of both sensation and evaluation. The present study aimed to discriminate the neural networks involved in identifying different temperature stimuli and the two different processes by using functional magnetic resonance imaging (fMRI). We applied four different thermal stimuli ("hot," 40C; "warm," 36 °C, "cool," 27 °C; and "cold," 22 °C) to the left forearm using Peltier apparatus. During the stimuli, participants were instructed to either evaluate (evaluation task) or not evaluate (no-evaluation task) and report the thermal sensation. We found brain activation in the medial prefrontal cortex/anterior cingulate gyrus, inferior frontal gyrus, bilateral insula, and posterior parietal cortex during the four thermal stimuli both with and without the evaluation task. Additionally, the stimuli with the evaluation task induced stronger and broader activation, including the right fronto-parietal and anterior insula regions. These results indicate that thermal stimulation activates the common neural networks, independent of the thermal conditions and evaluation process. Moreover, the evaluation process may increase the attention to the thermal stimuli, resulting in the activation of the right lateralized ventral attentional network.

1. Introduction

Conscious thermal perception is reportedly divided into thermal sensation (i.e., discriminative component) and thermal pleasantness/unpleasantness (i.e., hedonic component) (Cabanac, 1971; Hensel, 1981). Based on behavioral experiments, it is considered that the two components of thermal perception are processed independently. For example, Nakamura et al. (2008) reported that, in a hot environment, local cooling of the facial skin induced thermal comfort, but that of the abdominal skin induced thermal discomfort, although there were no regional differences in the thermal sensation.

The neural networks underlying thermal perception have been investigated by using neuroimaging approaches such as functional magnetic resonance imaging (fMRI) and positron emission tomography. These studies have indicated that the cingulate cortex, insula, thalamus, prefrontal cortex, primary and secondary somatosensory cortices, posterior parietal cortex, lentiform nucleus, midbrain, and retrosplenial cortex contribute to the discriminative component of the thermal perception as core neural networks (Casey et al., 1996; Craig et al., 2000; Davis et al., 1998; Egan et al., 2005; Oi et al., 2017; Olausson et al., 2005; Peltz et al., 2011; Tseng et al., 2010). Other studies have identified brain regions associated with the hedonic component of thermal perception, including the amygdala, mid-orbitofrontal/cingulate cortex, and ventral striatum (Farrell et al., 2011; Kanosue et al., 2002; Oi et al., 2017; Rolls et al., 2008).

We previously showed that different brain regions are involved in the discriminative and hedonic components, using an experimental paradigm that activated the two components separately (Aizawa et al., 2019). Several shared brain regions related to thermal sensation—such as the anterior cingulate cortex, insula, and inferior parietal lobe—were activated irrespective of the temperature of the local and whole-body thermal stimuli. Moreover, the evaluation process, which was conducted immediately after the local stimulus to assess thermal perception, activated brain regions such as the medial prefrontal cortex to the

Abbreviations: ANOVA, analysis of variance; fMRI, functional magnetic resonance imaging; FWE, family-wise error; FOV, field of view; MNI, Montreal Neurological Institute; TE, echo time; TR, repetition time; VAS, visual analog scale.

* Corresponding author.
E-mail addresses: k-nagashima@waseda.jp (K. Nagashima), hiroki-nakata@cc.nara-wu.ac.jp (H. Nakata), harada.tokiko.m3@f.mail.nagoya-u.ac.jp (T. Harada), kiki715im@akane.waseda.jp (I. Kato), sadato@nips.ac.jp (N. Sadato).

https://doi.org/10.1016/j.ibneur.2022.09.006
Received 12 May 2022; Accepted 17 September 2022
Available online 19 September 2022

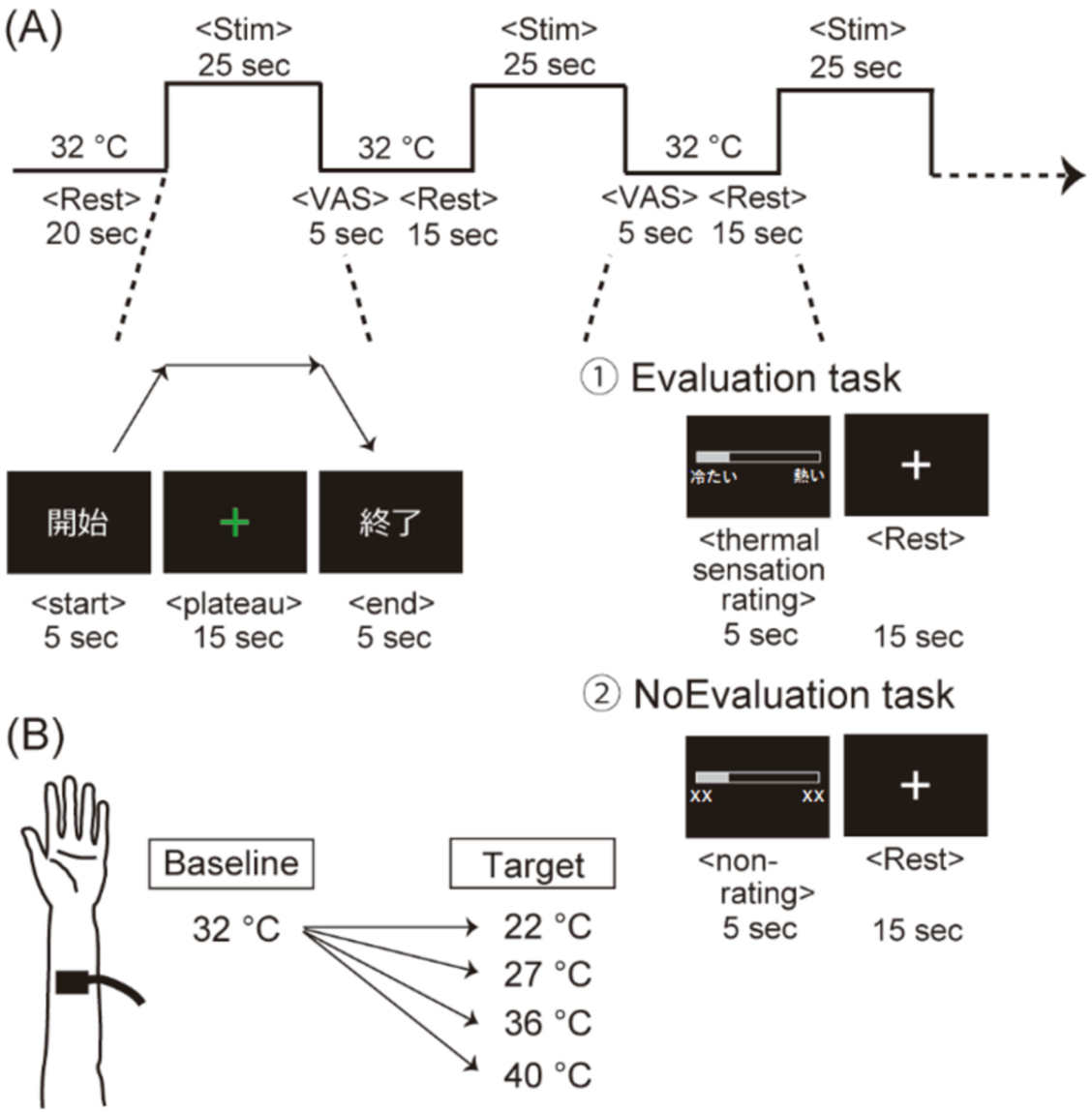

Fig. 1. (A) Scheme of experimental design. Each fMRI run consisted of 16 stimulation blocks with a 25-s duration each, interleaved with a 5-s evaluation and a 15-s rest periods. In the evaluation task, the participants were instructed to rate how cold or hot they perceived the thermal stimulation to be during the 15-s green cue. In the no-evaluation task, the participants were instructed to not rate the thermal stimulation and to move and stop a bar at an arbitrary position. (B) A thermal stimulus was delivered to the anterior plane of the left forearm with a Peltier apparatus. The thermode baseline temperature was set at 32 °C, and the target temperatures were 22 °C, 27 °C, 36 °C, and 40 °C.

anterior cingulate cortex, insula, middle frontal cortex, and parietal lobes, overlapping the brain regions activated during thermal stimuli. These results may suggest that thermal stimulation simultaneously activated the evaluation process. Furthermore, the evaluation process may have masked the brain activation reflecting the temperature of the local and whole-body thermal stimuli.

In daily life, temperature information arises from several parts of the body such as the skin, central nervous system, and visceral organs continuously and simulutaneously. This information is not always consciously accepted, which may characterize the nature of thermal perception, although the mechanism remains unclear. Previous fMRI studies that sought to clarify the neural networks associated with thermal perception, often instructed participants to evaluate thermal perception to the local and/or whole-body stimuli with psychophysical rating tools such as a point scale or visual analog scale (VAS). However, this evaluation process and/or the attention needed for the evaluation may have activated specific neural networks (e.g., attention network), which could be, at least partially, involved in the conscious acceptance of the thermal stimulus.

In this study, we aimed use fMRI to identify the neural networks involved in the discriminative component of thermal perception during thermal stimulus to the forearm. To exclude or assess the influence of the evaluation and/or attention process on the involved neural networks, we applied four different local thermal stimuli to the skin of the participants' forearms which induced hot, warm, cool, or cold sensations. Participants were instructed to both evaluate and report the thermal stimulus (evaluation task) and not do so (no-evaluation task). We hypothesized that 1) there are specific neural networks specific to the 4 different thermal stimuli, which are found during the stimuli with no-evaluation task, and 2) the evaluation task activates brain regions in addition to those associated with the thermal stimuli per se (i.e., thermal stimuli with no-evaluation task).

2. Materials and methods

2.1. Participants

Twenty-two healthy, right-handed, and non-smoking volunteers (11 men and 11 women; aged 26.0 ± 6.1 years (mean ± SD)) participated in the present study, in which all the participants were given local thermal stimulations to their left forearm. The participants received reimbursement for participating in the study. None of the participants had a history of neurological or psychiatric illness.

2.2. Thermal stimulation

A local thermal stimulation was applied to the anterior plane of the left forearm (Fig. 1). The local stimulation was delivered by a Peltier apparatus (3-cm diameter, covered with a thin copper board; Intercross 2000, Tokyo, Japan). The Peltier apparatus was attached to the skin surface with paper adhesion tape. The computer-controlled (LabVIEW 2013; National Instruments, Texas, USA) apparatus temperature was initially held at 32 °C for 20 s. Subsequently, the temperature underwent 25-s decrements to 22 °C or 27 °C (2 °C/s for the 25 s; i.e., the two local cold stimulation conditions) or increments to 36 °C or 40 °C (1.6 °C/s for the 25 s; i.e., the two local hot stimulation conditions). Baseline period consisting in 15-s 32 °C stimulation was added at the beginning and end of each experimental run and between trials, as the local temperature of 32 °C induces neither hot nor cold sensations (i.e., thermoneutral temperature) (Kingma et al., 2012).

2.3. Experimental procedure

All the 22 participants performed four experimental runs: two for the evaluation task (i.e., evaluation runs) and two for the no-evaluation task (i.e., no-evaluation runs). During the evaluation runs, local thermal stimulation was applied to the participants' left forearms, and they were instructed to rate the stimulation in terms of cold or hot. During the no-evaluation runs, local thermal stimulation was also applied to their left forearms, but they were instructed to not explicitly rate the stimulation. The four experimental runs were conducted in counterbalanced order across the participants.

In each experimental run, each of the four thermal conditions (i.e., 22 °C, 27 °C, 36 °C, and 40 °C) was repeated four times in a randomized order, with a baseline period of 32 °C stimulation inserted between trials. In each 25-s local thermal stimulation trial, the participants were given a 5-s start cue, a 15-s green fixation period, and a 5-s end cue. Within a subsequent 5-s evaluation period in the evaluation runs, the participants were instructed to rate how cold or hot they perceived the local thermal stimulation to be during the 15-s green cue with a VAS, indicating the left or right side of the VAS as very cold or very hot, respectively. The participants held a button box with their right hand and responded by pressing two buttons with their right index and middle fingers to move and stop a bar at an appropriate position on the VAS. Participants held a button box with their right hand and responded by pressing two buttons with their right index and middle fingers to move and stop a bar at an appropriate position on the VAS, with the bar continuously moving with every button press. In the no-evaluation runs, the participants were instructed not rate the thermal simulation and to move and stop a bar at an arbitrary position on the VAS. We included button pressing in the no-evaluation condition so we could subtract the neural activities related to it from those in the evaluation condition in the fMRI data analysis. A 15-s white fixation period was applied following the 5-s evaluation period, both at the temperature of 32 °C to serve as a baseline. (Fig. 1).

All visual stimuli were presented at the center of the screen by using Presentation software (Neurobehavioral Systems, Albany, CA). They were projected onto a half-transparent viewing screen located behind the MRI scanner head coil. The participants viewed the projected stimuli through a mirror attached to the head coil. Their responses were also recorded using Presentation software.

2.4. fMRI data acquisition

We used a 3-Tesla MRI scanner (MAGNETOM Verio, Siemens, Erlangen, Germany) equipped with a 32-channel phased array head coil. Functional brain images were obtained in an axial-oblique position covering the whole brain with a multiband Echo-Planar Imaging sequence (Moeller et al., 2010) (repetition time (TR) = 1000 ms; echo time (TE) = 35 ms; flip angle = 63°; field of view (FOV) = 192 mm^2; 60 slices; in-plane resolution = 2 × 2 mm; slice thickness = 2.5 mm including 0.5 mm gap; and multiband factor = 6) that was sensitive to blood-oxygen-level-dependent contrast. The number of T2 * -weighted images was 740 for each fMRI run. A high-resolution anatomical T1-weighted image (MPRAGE; TR = 1.8 s; TE = 1.98 ms; flip angle = 9°; FOV = 256 mm^2; 176 slices; and voxel size = 1 × 1 × 1 mm) was also acquired for each participant. Foam padding was placed around each participant's head to minimize head movement.

2.5. Statistical analysis of psychological data

Participants' VAS scores were recorded as a range from − 50 to + 50 indicating very cold or very hot, respectively. We calculated the mean VAS scores for each task and thermal conditions for each participant. The VAS scores of the thermal sensation in the left forearm were submitted to two-way analysis of variance (ANOVA) with repeated-measures using task (evaluation and no-evaluation) and thermal condition (22 °C, 27 °C, 36 °C, and 40 °C) as within-subjects factors. In all repeated-measures factors with more than two levels, we tested whether Mauchly's sphericity assumption was violated. If the result of Mauchly's test was significant and the assumption of sphericity was violated, the Greenhouse-Geisser adjustment was used to correct sphericity by altering the degrees of freedom using a correction coefficient epsilon. When a significant main effect was identified, Bonferroni post-hoc multiple comparison tests were conducted to evaluate differences among conditions. Statistical evaluations were performed using the IBM SPSS Statistics 22 software (IBM, Chicago, USA). All values are presented as means ± SD, and significant difference was set at a level of $p < 0.05$.

2.6. fMRI data analysis

The MRI data were analyzed with SPM8 software (Wellcome Department of Imaging Neuroscience, London, UK) implemented in MATLAB R2012a (MathWorks, Sherborn, MA, USA). The first ten volumes were discarded due to unsteady magnetization, and all the remaining images were spatially realigned to the mean image. After a high-resolution image was co-registered onto the mean image, all volumes were normalized to the Montreal Neurological Institute (MNI) space (using the MNI template) using a transformation matrix obtained from the normalization process of the high-resolution image of each individual participant to the MNI template. The normalized and resliced images were then spatially smoothed with Gaussian kernel of 8 mm (full width at half-maximum) in the x, y, and z axes.

After preprocessing, statistical analysis for each participant was conducted using a general linear model (Friston et al., 1995). At the first level, the 5-s first period (i.e., the onset period), the 10-s middle period running from 8 s to 18 s (i.e., the sustained period), and the 5-s last period (i.e., the offset period) of the 20-s local thermal stimulation were modeled separately for each of the four thermal stimulation conditions (i.e., 22 °C, 27 °C, 36 °C, and 40 °C), convolving a hemodynamic response function. In the present study, we focused on the 10-s middle period (i.e., the sustained period), in which the temperature of the local thermal stimulation remained stable. The period of explicit evaluation of the thermal sensation (for the evaluation runs) or that of simply moving

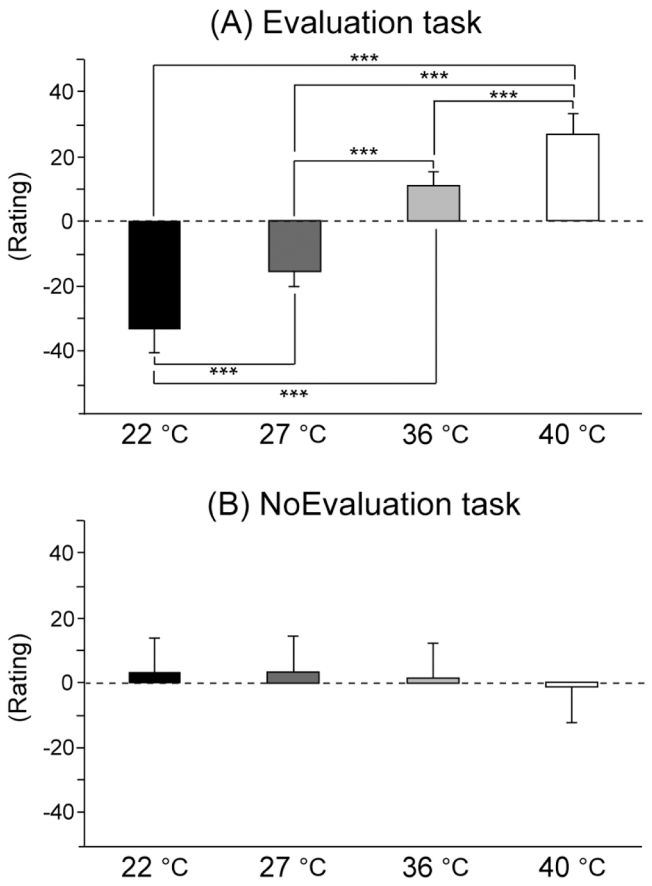

Fig. 2. Thermal sensation ratings for the left forearm in the (A) evaluation and (B) no-evaluation tasks. The x-axis indicates the temperature of the thermal stimuli and the y-axis indicates the mean VAS scores (−50 and +50 as very cold and very hot, respectively) using an arbitrary unit. * ** : $p < 0.001$.

a bar on the VAS without subjective rating (for the no-evaluation runs) was also modeled separately with a 5-s duration, convolving a hemodynamic response function. Furthermore, six regressors for movement parameters obtained in the realignment process were entered in the design matrix. An additional regressor of the mean signal from the cerebrospinal fluid was also included in the design matrix. High-pass filters (128 s) were applied to the time-series data. An autoregressive model was used to estimate the temporal autocorrelation. The image signals were scaled to a grand mean of 100 overall voxels and volumes within each run. For each of the evaluation and no-evaluation condition, the parameter estimate for the 10-s sustained period of local thermal stimulation was computed for each of the four thermal stimulation conditions from the least-square fit of the model to the time-series data at each voxel. For the period of explicit evaluation of the thermal sensation (for the evaluation runs) or that of simply moving a bar on the VAS without subjective rating (for the no-evaluation runs), the parameter estimate was computed combining all the four thermal stimulation conditions. Images of the parameter estimates representing related neural activities (i.e., contrast images) were created for each participant.

In the second-level analysis, the contrast images obtained from each participant were entered into the group analyses with a random-effect model. First, to examine whether local thermal stimulation with a given temperature was processed in dissociable brain regions and whether the evaluation and no-evaluation runs involved different brain regions, a one-way within-subjects ANOVA was conducted with the contrast images pertaining to the four thermal stimulation conditions for the evaluation and no-evaluation runs. To examine shared brain regions between the evaluation and no-evaluation runs, a conjunction analysis was also performed including all four thermal stimulation conditions together. The statistical thresholds were set at uncorrected $p = 0.001$ for multiple comparisons at the voxel level, and at family-wise error (FWE)-corrected $p = 0.05$ for multiple cluster-level comparisons (Slotnick, 2017). All the coordinates were reported in the MNI space. Brodmann areas and brain regions were identified based on the Talairach Atlas (Talairach and Tournoux, 1988) after converting MNI coordinates to Talairach space with a nonlinear transformation. To identify differences in activated brain regions during the thermal stimuli with the evaluation and no-evaluation tasks, one-way ANOVA with within-subject factor was applied.

3. Results

3.1. Rating of thermal sensation

Fig. 2 shows the rating of thermal sensation in the forearm for the evaluation and no-evaluation tasks. ANOVA analysis showed significant main effects for task ($F(1, 21) = 8.108$, $p < 0.05$) and condition ($F(3, 63) = 109.133$, $p < 0.001$) and task-condition interactions (Greenhouse-Geisser correction: $F(1.724, 36.194) = 85.357$, $p < 0.001$, $\square = 0.575$). The post-hoc test demonstrated that the rating of thermal sensation for the evaluation task was significantly higher in the 40 °C condition compared to the 22 °C, 27 °C, and 36 °C conditions ($p < 0.001$). It was also significantly higher in the 36 °C condition compared to the 22 °C and 27 °C conditions ($p < 0.001$) and in the 27 °C condition compared to the 22 °C condition ($p < 0.001$). These differences were not observed for the no-evaluation task.

3.2. fMRI results

During thermal stimuli with the evaluation task, neural networks including the medial prefrontal cortex/anterior cingulate gyrus, inferior frontal gyrus, bilateral insula, and posterior parietal cortex (superior and inferior parietal lobules) were involved across all thermal conditions (Table 1 and Fig. 3A). Similar brain regions were activated during the no-evaluation task (Table 1 and Fig. 3B). Conjunction analysis for activated regions in common during the evaluation and no-evaluation tasks revealed significant activation in the neural networks (Table 2 and Fig. 4C).

We found differences in activated brain regions during the evaluation and no-evaluation tasks related to the thermal stimuli. Activities in the right inferior/middle frontal gyrus, anterior insula, and posterior parietal cortex were significantly stronger during the evaluation compared to the no-evaluation task (Table 3 and Fig. 4).

We also found significantly less brain activation in the right anterior insula for the 40 °C compared to 22 °C stimuli, and the dorsal medial prefrontal cortex and the left inferior frontal gyrus for the 40 °C compared to 36 °C stimuli in the no-evaluation task (Table 4). There was no significant difference in brain activity among the 4 different thermal stimuli in the evaluation task. We found that brain activation during the 40 °C stimuli was significantly smaller in the no-evaluation task compared to the evaluation task (Table 4).

4. Discussion

This study investigated differences in the neural networks activated during local stimulus with and without an evaluation task using fMRI. We applied local hot (40 °C), warm (36 °C), cool (27 °C), or cold (22 °C) stimuli to the left forearm and asked participants to evaluate or to not evaluate the thermal sensation. A common brain network was activated for the four different thermal stimuli whether or not an explicit evaluation was required. However, there was no brain region specific to each of the four different thermal stimuli, but there was less activation for the 40 °C condition in the no-evaluation task. We also found broader and/or stronger activities in a right-lateralized brain network during the thermal stimuli with the evaluation task.

Table 1
Brain regions involved in perception of four thermal local stimuli to the left forearm during the evaluation and no-evaluation tasks.

FWE-corrected p-value (cluster-level)	Cluster size (voxels)	Z-value (peak-level)	x (mm)	y (mm)	z (mm)	BA	Brain area
Evaluation task							
22 °C							
<0.001	6663	7.68	34	18	4		Rt. anterior insula
	*	7.56	62	-18	18	43	Rt. postcentral gyrus
	*	7.17	42	2	-2		Rt. posterior insula
	*	5.57	52	12	12	44	Rt. inferior frontal gyrus
	*	5.48	56	-34	46	40	Rt. inferior parietal lobe
	*	5.36	44	48	0	10/46	Rt. inferior/middle formal gyrus
	*	5.34	24	34	-14	11	Rt. middle frontal gyrus
<0.001	3664	6.79	-34	18	8		Lt. anterior insula
	*	6.10	-42	-4	0		Lt. posterior insula
	*	5.99	-22	30	-14	11	Lt. middle frontal gyrus
	*	5.35	-44	46	6	10/46	Lt. inferior/middle formal gyrus
	*	4.21	-48	4	14	44	Lt. inferior frontal gyrus
<0.001	2191	7.07	4	22	50	6/32	Rt. medial frontal gyrus/anterior cingulate gyrus
	*	4.57	-8	28	46	6/32	Lt. medial frontal gyrus/anterior cingulate gyrus
0.002	454	5.89	-64	-20	20	43	Lt. postcentral gyrus
0.022	280	4.29	-36	-54	46	7	Lt. superior parietal lobe
27 °C							
<0.001	1830	6.67	-8	4	58	6/32	Lt. medial frontal gyrus/anterior cingulate gyrus
	*	6.28	8	14	52	6/32	Rt. medial frontal gyrus/anterior cingulate gyrus
<0.001	1596	5.42	54	10	8	44	Rt. inferior frontal gyrus
	*	4.51	32	18	8		Rt. anterior insula
	*	4.38	48	38	8	10/46	Rt. inferior/middle formal gyrus
	683	5.46	-32	18	8		Lt. anterior insula
	*	4.33	-54	8	10	44	Lt. inferior frontal gyrus
	640	4.94	50	-32	40	40	Rt. inferior parietal lobe
	*	4.29	44	-42	58	7	Rt. superior parietal lobe
36 °C							
<0.001	9907	Inf	6	20	48	6/32	Rt. medial frontal gyrus/anterior cingulate gyrus
	*	7.63	-4	8	54	6/32	Lt. medial frontal gyrus/anterior cingulate gyrus
	*	7.62	34	22	4		Rt. anterior insula
	*	7.22	50	10	22	44	Rt. inferior frontal gyrus
	*	6.11	42	2	40	6	Rt. precentral gyrus
	*	5.92	62	-18	24	43	Rt. postcentral gyrus
	*	5.87	40	-46	48	40	Rt. inferior parietal lobe
	*	4.51	46	42	8	10/46	Rt. inferior/middle formal gyrus
<0.001	2646	Inf	-32	16	8		Lt. anterior insula
	*	5.07	-48	6	26	44	Lt. inferior frontal gyrus
	*	3.56	-44	42	8	10/46	Lt. inferior/middle formal gyrus
<0.001	1332	6.15	-34	-52	44	40	Lt. inferior parietal lobe
40 °							
<0.001	6786	6.97	60	-16	16	43	Rt. postcentral gyrus
	*	6.66	34	20	6		Rt. anterior insula
	*	6.26	52	14	18	44	Rt. inferior frontal gyrus
	*	5.75	52	-32	46	40	Rt. inferior parietal lobe
	*	4.74	44	44	8	10/46	Rt. inferior/middle formal gyrus
<0.001	3205	7.38	-32	16	8		Lt. anterior insula
	*	5.56	-54	8	10	44	Lt. inferior frontal gyrus
	*	4.26	-60	-20	18	43	Lt. postcentral gyrus
<0.001	2281	7.04	6	20	48	6/32	Rt. medial frontal gyrus/anterior cingulate gyrus
	*	4.14	-6	24	34	6/32	Lt. medial frontal gyrus/anterior cingulate gyrus
<0.001	665	5.36	-48	-32	44	40	Lt. inferior parietal lobe
The no-evaluation task							
22 °C							
<0.001	3394	7.11	-36	14	6		Lt. insula
	*	5.00	-50	14	-4	44	Lt. inferior frontal gyrus
	*	4.58	-42	46	10	10/46	Lt. inferior/middle formal gyrus
<0.001	2698	5.91	4	20	50	6/32	Rt. medial frontal gyrus/anterior cingulate gyrus
	*	5.19	-2	24	36	6/32	Lt. medial frontal gyrus/anterior cingulate gyrus
<0.001	2200	6.28	44	-4	0		Rt. posterior insula
	*	5.92	36	16	4		Rt. anterior insula
	*	4.79	56	14	4	44	Rt. inferior frontal gyrus
<0.001	892	4.76	-54	-40	40	40	Lt. inferior parietal lobe
<0.001	852	4.85	56	-24	18	43	Rt. postcentral gyrus
	*	4.32	54	-30	38	40	Rt. inferior parietal lobe
0.041	235	3.74	36	46	24	10/46	Rt. inferior/middle formal gyrus
27 °C							
<0.001	2181	6.46	-2	6	54	6/32	Lt. medial frontal gyrus/anterior cingulate gyrus
	*	5.56	2	16	44	6/32	Rt. medial frontal gyrus/anterior cingulate gyrus
<0.001	2095	5.74	50	6	2	44	Rt. inferior frontal gyrus
	*	5.17	32	22	10		Rt. anterior insula

(*continued on next page*)

Table 1 (*continued*)

FWE-corrected p-value (cluster-level)	Cluster size (voxels)	Z-value (peak-level)	x (mm)	y (mm)	z (mm)	BA	Brain area
	*	4.69	62	-28	20	43	Rt. postcentral gyrus
<0.001	826	5.84	-34	14	8		Lt. anterior insula
	*	5.45	-56	8	4	44	Lt. inferior frontal gyrus
0.004	410	4.64	-32	52	22	10	Lt. middle frontal gyrus
36 °C							
<0.001	3823	7.25	-38	14	6		Lt. anterior insula
	*	6.48	-48	14	0	44	Lt. inferior frontal gyrus
	*	5.56	-38	30	26	9/46	Lt. middle frontal gyrus
<0.001	2985	6.25	0	20	48	6/32	medial frontal gyrus/anterior cingulate gyrus
<0.001	1461	4.79	56	14	6	44	Rt. inferior frontal gyrus
	*	4.54	38	22	6		Rt. anterior insula
0.004	404	4.91	-56	-42	42	40	Lt. inferior parietal lobe
0.033	250	4.67	32	-66	-34		Rt. cerebellum
40 °C							
0.001	553	4.33	-2	22	44	6/32	Lt. medial frontal gyrus/anterior cingulate gyrus
0.003	426	4.97	-14	-70	50	7	Lt. superior parietal lobe
0.009	347	4.58	-34	-54	46	40	Lt. inferior parietal lobe

Coordinates (x, y, z) are of the voxel of local maximal significance in each brain region, according to the Montreal Neurological Institute (MNI) template. Brain areas were identified based on the stereotaxic coordinate system of Talairach and Tournoux (1988). Voxel dimension = 2 × 2 × 2 mm. * , a peak was included in a large cluster. BA, Brodmann Area; FWE, family-wise error; Lt., left brain hemisphere; Rt., right brain hemisphere.

4.1. Psychological assessment

Psychological assessment has been conducted in many previous studies of thermal perception. For example, the thermal sensation of local heat or cold (i.e., discriminative component) is initially determined by the skin temperature, without the influence of the core body temperature or environmental conditions (i.e., hot or cold) (Attia, 1984; Cabanac, 1971; Chatonnet and Cabanac, 1965; Kuno, 1987; Mower, 1976; Nakamura et al., 2008, 2013). Similarly, in the present study we conducted the evaluation task using VAS while the four thermal stimulations were administered to the participants' left forearms. In the evaluation task, the ratings significantly differed among the 22 °C, 27 °C, 36 °C, and 40 °C conditions. However, in the no-evaluation task, no significant differences were observed among the different conditions. These results indicated that the participants could adequately classify the thermal sensation in the evaluation task, while they randomly selected the VAS ratings in the no-evaluation task. These psychological data supported the differences in fMRI findings between the evaluation and no-evaluation tasks.

4.2. Differences in brain activities between the evaluation and no-evaluation tasks

We found stronger brain activation in the right fronto-parietal and anterior insula regions during thermal stimulation with than without the task (Table 3 and Fig. 4). These activations may be related to a key component of the right-lateralized ventral attention network that includes structures such as the inferior frontal gyrus and posterior parietal cortex (Corbetta et al., 2008; Kucyi et al., 2012; Ptak, 2012). Anatomically, a diffusion-weighted MRI study has shown a larger fronto-parietal

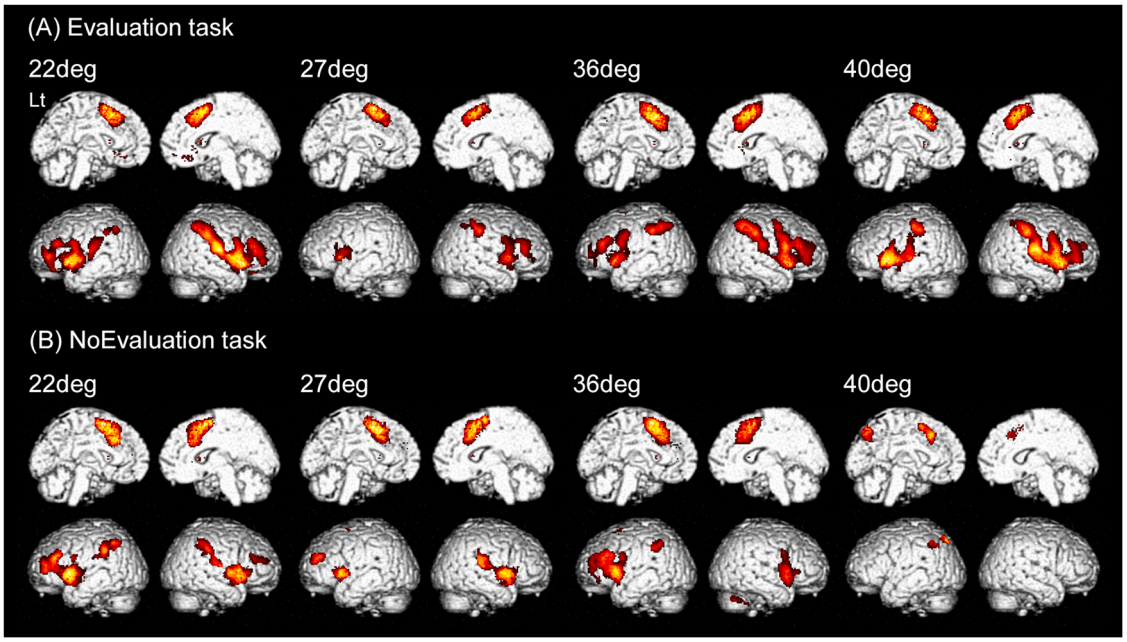

Fig. 3. Brain regions activated under the four thermal stimulation conditions (i.e., 22 °C, 27 °C, 36 °C, and 40 °C) as rendered on the medial and lateral surfaces of the brain for the (A) evaluation task and(B) no-evaluation task. The statistical threshold was set to uncorrected $p < 0.001$ at the voxel level and to FWE-corrected $p < 0.05$ for multiple cluster-level comparisons. Lt indicates the left side of the brain.

Table 2
Shared brain regions in the evaluation and no-evaluation tasks.

FWE-corrected p-value (cluster-level)	Cluster size (voxels)	Z-value (peak-level)	x (mm)	y (mm)	z (mm)	BA	Brain area
<0.001	4450	6.89	56	12	2	44	Rt. inferior frontal gyrus
	*	6.67	36	20	8		Rt. anterior insula
	*	5.46	64	-18	14	43	Rt. postcentral gyrus
	*	5.04	52	-36	44	40	Rt. inferior parietal lobe
<0.001	4155	Inf	-38	14	6		Lt. anterior insula
	*	7.29	-48	12	0	44	Lt. inferior frontal gyrus
	*	5.03	-34	54	10	10/46	Lt. inferior/middle formal gyrus
<0.001	3510	Inf	0	20	48	6/32	Medial frontal gyrus/anterior cingulate gyrus
		4.24	28	4	50	6	Rt. precentral gyrus
<0.001	1124	6.39	-34	-52	44	7	Lt. superior parietal lobe
	*	5.68	-48	-40	38	40	Lt. inferior parietal lobe

Coordinates (x, y, z) are of the voxel of local maximal significance in each brain region, according to the Montreal Neurological Institute (MNI) template. Brain areas were identified based on the stereotaxic coordinate system of Talairach and Tournoux (1988). Voxel dimension = 2 × 2×2 mm. * , a peak was included in a large cluster. BA, Brodmann Area; FWE, family-wise error; Lt., left brain hemisphere; Rt., right brain hemisphere.

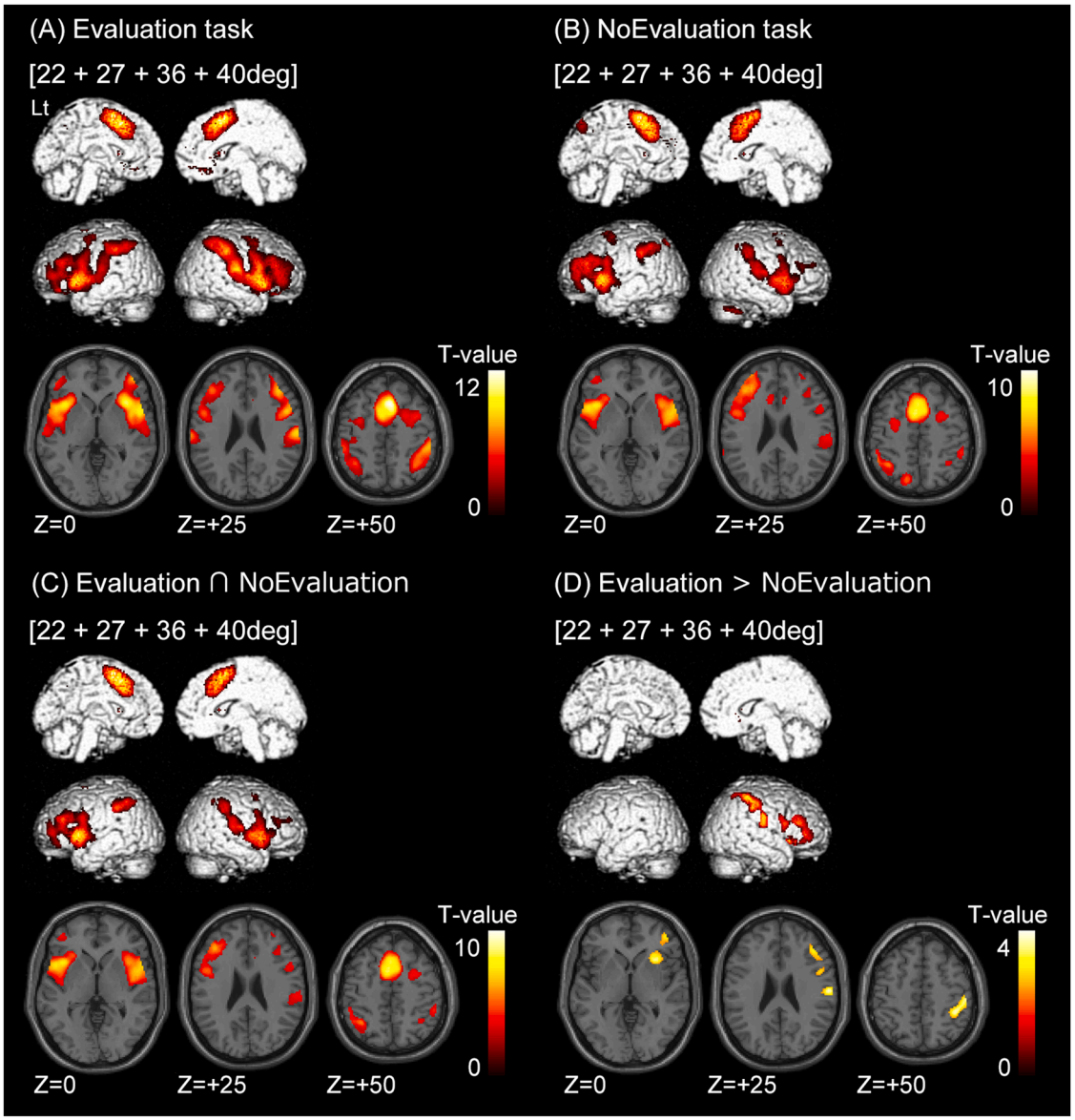

Fig. 4. Brain regions activated across the four thermal stimulation conditions as rendered on the medial and lateral surfaces of the brain and superimposed onto axial sections (Z = 0, 25 and 50 mm) of an SPM standard brain for the (A) evaluation task and (B) no-evaluation task. (C) Shared activated brain regions across the two tasks and (D) more activated regions for the evaluation task compared to the no-evaluation task as rendered on the medial and lateral surfaces of the brain and superimposed onto axial sections (Z = 0, 25 and 50 mm) of an SPM standard brain. The statistical threshold was set to uncorrected $p < 0.001$ at the voxel level and FWE-corrected $p < 0.05$ for multiple comparisons for (A), (B), and (C). The statistical threshold was set to uncorrected $p < 0.005$ at the voxel level and FWE-corrected $p < 0.05$ for multiple cluster-level comparisons for (D).

Table 3
Brain regions more activated in the evaluation task compared to the no-evaluation task.

FWE-corrected p-value (cluster-level)	Cluster size (voxels)	Z-value (peak-level)	x (mm)	y (mm)	z (mm)	BA	Brain area
0.001	1083	3.93	32	18	-2		Rt. anterior insula
	*	3.75	42	34	22	10/46	Rt. inferior/middle frontal gyrus
	*	3.45	52	12	18	44	Rt. inferior frontal gyrus
0.002	1006	4.17	42	-40	56	7	Rt. superior parietal lobe†

The statistical threshold was set to uncorrected $p < 0.005$ at the voxel level and family-wise error (FWE)-corrected $p < 0.05$ for multiple cluster-level comparisons. †, a significantly activated region at uncorrected $p < 0.001$ at the voxel level and FWE-corrected $p < 0.05$ for multiple cluster-level comparisons.

network in the right than in the left hemisphere, and a significant correlation between the degree of anatomical lateralization and the asymmetry of performance on visuospatial tasks (Thiebaut de Schotten et al., 2011). Further, some previous studies have reported right-lateralized processing for pain stimulation, regardless of the side of stimulation (Coghill et al., 2001; Symonds et al., 2006).

However, in previous neuroimaging studies, the participants evaluated thermal perception through psychophysical rating tools such as VAS and pleasantness/unpleasantness ratings, and fMRI data were recorded while the thermal stimulation was administered. These findings may suggest that the activated neural networks were influenced by attention to the thermal stimulus. Indeed, several studies have reported that the right-lateralized regions involved in thermal stimulation include the middle frontal gyrus, anterior cingulate, inferior frontal gyrus, medial/superior frontal gyri, and inferior parietal lobule (Coghill et al., 2002; Symonds et al., 2006). This is consistent with our findings for the stimulus with the evaluation task (Table 3 and Fig. 4). Additionally, the reduced brain activation during the 40 °C stimulus with the no-evaluation task may have reflected the difference in attention levels between temperatures (i.e., the cold stimulus induces greater attention than the warm stimulus, even when the evaluation task was not conducted). Since we only observed right-lateralized processing in the thermal stimuli with the evaluation task, we propose that the findings in previous neuroimaging studies that indicated right-lateralized processing reflected the influence of the evaluation process rather than the thermal (pain) stimulation per se. This notion might be supported by Bingel et al. (2003). They recorded fMRI during pain laser stimulation to the left or right hand and did not request participants to rate the perceived pain intensity. They reported no hemispheric lateralization, irrespective of the stimulated hand.

We also found greater activation in the anterior insula during thermal stimulus with the evaluation task. The anterior insular exhibits functional properties that are not limited to pain and emotional processing but also encompass various cognitive processes such as attention (Corbetta et al., 2008), saliency (Menon and Uddin, 2010), human body scheme representation (Karnath and Baier, 2010), social interactions expressed by gaze (Ethofer et al., 2011), and social empathy (for meta-analyses, see Kurth et al., 2010). The anterior insula is also involved in the ventral attention network, and a rightward asymmetry in connectivity strength between the posterior parietal cortex and insula was reported (Kucyi et al., 2012). Based on these findings, since the anterior insular plays an important integrative role in human cognitive function, it is not surprising that the anterior insula showed greater activity during the thermal stimulus with the evaluation task in this study.

Our previous study using fMRI also showed the activation of brain regions during the evaluation of thermal sensation, which was conducted after thermal stimulation (Aizawa et al., 2019). This study identified more activated brain regions during the thermal stimuli with the evaluation task than that with no-evaluation task. Therefore, this is the first study to show that the attention to thermal stimulus induces greater and broader activation of the brain regions involved in thermal sensation.

4.3. Shared regions activated during the evaluation and no-evaluation tasks

In the four trials with the evaluation task (i.e., 22 °C, 27 °C, 36 °C, and 40 °C), the neural networks involved the medial prefrontal cortex/anterior cingulate gyrus, inferior frontal gyrus, bilateral insula, and

Table 4
Difference in brain region activity among the different local thermal stimuli.

FWE-corrected p-value (cluster-level)	Cluster size (voxels)	Z-value (peak-level)	x (mm)	y (mm)	z (mm)	BA	Brain area
No-evaluation task							
22 °C > 40 °C with an inclusive mask of 22 °C (uncorrected $p < 0.001$ at the voxel level)							
0.002	476	4.19	40	12	6		Rt. anterior insula
No-evaluation task							
36 °C > 40 °C with an inclusive mask of 36 °C (uncorrected $p < 0.001$ at the voxel level)							
0.023	277	3.94	4	12	60	8	Rt. medial frontal gyrus
0.047	225	4.37	-42	16	8	44/45	Lt. inferior frontal gyrus
40 °C							
Evaluation task > No-evaluation task with an inclusive mask of Evaluation task (uncorrected $p < 0.001$ at the voxel level)							
<0.001	969	4.30	38	18	-8		Rt. anterior insula
0.003	448	4.09	54	-16	30	1	Rt. postcentral gyrus
	*	4.00	60	-12	14	43	Rt. postcentral gyrus
	*	3.71	42	-36	48	40	Rt. inferior parietal lobe

Coordinates (x, y, z) are of the voxel of local maximal significance in each brain region, according to the Montreal Neurological Institute (MNI) template. Brain areas were identified based on the stereotaxic coordinate system of Talairach and Tournoux (1988). Voxel dimension = 2×2 x 2 mm. * , a peak was included in a large cluster. BA, Brodmann Area; FWE, family-wise error; Lt., left brain hemisphere; Rt., right brain hemisphere.

posterior parietal cortex (superior and inferior parietal lobules). Similar brain regions were activated in trials with no- evaluation task. Therefore, these regions may reflect the basic neural mechanism involved in thermal sensation. The activated brain regions identified in the present study mostly coincide with those in previous reports (Becerra et al., 1999; Casey et al., 1996; Craig et al., 2000; Hua et al., 2005).

An interesting point was that the neural networks were independent of the degree of thermal temperature delivered to the left forearm. This indicates that even if the participants perceived a cold or hot sensation from the thermal stimulation, the basic neural activities were almost the same. Another possibility is that fMRI recording cannot dissociate the neural activities between cold and hot stimuli. In our previous fMRI study (Aizawa et al., 2019), we applied a local thermal stimulus of either 41.5 °C or 18.0 °C to the left forearm during a whole-body thermal stimulus of 47.0 °C, 32.0 °C, or 17.0 °C. Local thermal stimulation activated specific brain regions such as the anterior cingulate cortex, insula, and inferior parietal lobe, irrespective of the temperature of the local and whole-body stimuli. However, no specific activation corresponding to hot or cold sensations was observed, indicating the current limitation in fMRI research on thermal sensation.

4.4. *Different brain activities between temperatures of the thermal stimuli*

Despite the similar brain activity during the four different thermal stimuli with the evaluation task, we found decreased brain activations during the 40 °C stimulus compared to both the 22 °C and the 36 °C stimuli in the no-evaluation task (Table 4). These regions include the right anterior insula, left inferior frontal gyrus, and dorsal medial prefrontal cortex, which overlapped with the brain regions commonly activated for the four different thermal stimuli. We speculate that the cold stimulus automatically induced greater attention than the hot stimulus when an explicit evaluation was not required. However, the evaluation task may have strongly activated the attention neural networks in the same manner among the four thermal stimuli, decreasing the specific influence of the stimulating temperature. Still, more elaborative research is needed to verify this speculation.

4.5. *Limitations of the present study*

In the present study, we applied local hot, warm, cool, or cold stimuli to the left forearm and instructed the participants to evaluate or not to evaluate the thermal sensation. To the best of our knowledge, no previous neuroimaging studies on the thermal sensation have examined the difference in body sides between the left and right forearms (hand), even though many pain studies have reported hemispheric lateralization on the pain matrix (Bingel et al., 2003; Coghill et al., 2001; Schlereth et al., 2003; Symonds et al., 2006; Youell et al., 2004). Further studies are needed to clarify this issue.

5. Conclusion

The present study compared the neural networks during thermal stimulus where the participants evaluated or did not evaluate the thermal sensation delivered to the left forearm. We clarified that thermal stimulation activated the medial prefrontal cortex/anterior cingulate gyrus, inferior frontal gyrus, bilateral insula, and posterior parietal cortex, irrespective of the temperature of thermal stimulus, whether or not the explicit evaluation process was required. Furthermore, the evaluation task involved stronger and broader brain activation in the regions. The regions included the right fronto-parietal and anterior insula regions, which may be involved in a right-lateralized attention network mechanism. Such a response may enhance our thermal perception, such as discriminating the temperature of materials and/or living environment.

Funding sources

This study was supported by the Cooperative Study Program of the National Institute for Physiological Sciences and by a Japan Society for the Promotion of Science KAKENHI Grant-in-Aid for Scientific Research A 19H01128.

Compliance with ethical standards

All the participants gave their written informed consent for the experimental protocol, which was approved by the Human Research Ethics Committee of Waseda University and the National Institute for Physiological Sciences. The experiments were conducted in accordance with the Declaration of Helsinki.

CRediT authorship contribution statement

K.N. and **S.N.** substantially contributed to the study conceptualization. **H.N., T.H.** and **K.N.** designed the study. **H.N., T.H. I.K.** and **K.N.** performed the experiments, analyzed the data, and wrote the manuscript. All authors critically reviewed and revised the manuscript draft and approved the final version for submission.

Author contributions

K.N. and **S.N.** supervised the entire project. **H.N., T.H.** and **K.N.** designed the study, **H.N., T.H. I. K.** and **K.N.** performed the experiments, analyzed the data, and wrote the manuscript.

Declaration of interest

None.

Acknowledgements

Na.

References

Aizawa, Y., Harada, T., Nakata, H., Tsunakawa, M., Sadato, N., Nagashima, K., 2019. Assessment of brain mechanisms involved in the processes of thermal sensation, pleasantness/unpleasantness, and evaluation. IBRO Rep. 6, 54–63. https://doi.org/10.1016/j.ibror.2019.01.003.

Attia, M., 1984. Thermal pleasantness and temperature regulation in man. Neurosci. Biobehav. Rev. 8, 335–342. https://doi.org/10.1016/0149-7634(84)90056-3.

Becerra, L.R., Breiter, H.C., Stojanovic, M., Fishman, S., Edwards, A., Comite, A.R., Gonzalez, R.G., Borsook, D., 1999. Human brain activation under controlled thermal stimulation and habituation to noxious heat: an fMRI study. Magn. Reson. Med. 41, 1044–1057. https://doi.org/10.1002/(sici)1522-2594(199905)41:5%3C1044::aid-mrm25%3E3.0.co;2-m.

Bingel, U., Quante, M., Knab, R., Bromm, B., Weiller, C., Büchel, C., 2003. Single trial fMRI reveals significant contralateral bias in responses to laser pain within thalamus and somatosensory cortices. Neuroimage 18, 740–748. https://doi.org/10.1016/s1053-8119(02)00033-2.

Cabanac, M., 1971. Physiological role of pleasure. Science 173, 1103–1107. https://doi.org/10.1126/science.173.4002.1103.

Casey, K.L., Minoshima, S., Morrow, T.J., Koeppe, R.A., 1996. Comparison of human cerebral activation pattern during cutaneous warmth, heat pain, and deep cold pain. J. Neurophysiol. 76, 571–581. https://doi.org/10.1152/jn.1996.76.1.571.

Chatonnet, J., Cabanac, M., 1965. The perception of thermal comfort. Int. J. Biometeorol. 9, 183–193. https://doi.org/10.1007/BF02188475.

Coghill, R.C., Gilron, I., Iadarola, M.J., 2001. Hemispheric lateralization of somatosensory processing. J. Neurophysiol. 85, 2602–2612. https://doi.org/10.1152/jn.2001.85.6.2602.

Corbetta, M., Patel, G., Shulman, G.L., 2008. The reorienting system of the human brain: from environment to theory of mind. Neuron 58, 306–324. https://doi.org/10.1016/j.neuron.2008.04.017.

Craig, A.D., Chen, K., Bandy, D., Reiman, E.M., 2000. Thermosensory activation of insular cortex. Nat. Neurosci. 3, 184–190. https://doi.org/10.1038/72131.

Davis, K.D., Kwan, C.L., Crawley, A.P., Mikulis, D.J., 1998. Functional MRI study of thalamic and cortical activations evoked by cutaneous heat, cold, and tactile stimuli. J. Neurophysiol. 80, 1533–1546. https://doi.org/10.1152/jn.1998.80.3.1533.

Egan, G.F., Johnson, J., Farrell, M., McAllen, R., Zamarripa, F., McKinley, M.J., Lancaster, J., Denton, D., Fox, P.T., 2005. Cortical, thalamic, and hypothalamic

responses to cooling and warming the skin in awake humans: a positron-emission tomography study. Proc. Natl Acad. Sci. USA., 102, 5262–5267. ⟨https://dx.doi.org/10.1073%2Fpnas.0409753102⟩.
Ethofer, T., Gschwind, M., Vuilleumier, P., 2011. Processing social aspects of human gaze: a combined fMRI-DTI study. Neuroimage 55, 411–419. https://doi.org/10.1016/j.neuroimage.2010.11.033.
Farrell, M.J., Johnson, J., McAllen, R., Zamarripa, F., Denton, D.A., Fox, P.T., Egan, G.F., 2011. Brain activation associated with ratings of the hedonic component of thermal sensation during whole-body warming and cooling. J. Therm. Biol. 36, 57–63 https://dx.doi.org/10.4161%2Ftemp.29667.
Friston, K.J., Holmes, A.P., Worsley, K.J., Poline, J.-P., Frith, C.D., Frackowiak, R.S.J., 1995. Spatial parametric maps in functional imaging: a general linear approach. Hum. Brain Mapp. 2, 189–210. https://doi.org/10.1002/hbm.460020402.
Hensel, H., 1981. Thermoreception and temperature regulation. Monogr. Physiol. Soc. 38, 1–321.
Hua, le H., Strigo, I.A., Baxter, L.C., Johnson, S.C., Craig, A.D.B., 2005. Anteroposterior somatotopy of innocuous cooling activation focus in human dorsal posterior insular cortex. Am. J. Physiol. Regul. Integr. Comp. Physiol. 289, R319–R325.
Kanosue, K., Sadato, N., Okada, T., Yoda, T., Nakai, S., Yoshida, K., Hosono, T., Nagashima, K., Yagishita, T., Inoue, O., Kobayashi, K., Yonekura, Y., 2002. Brain activation during whole body cooling in humans studied with functional magnetic resonance imaging. Neurosci. Lett. 329, 157–160. https://doi.org/10.1016/S0304-3940(02)00621-3.
Karnath, H.O., Baier, B., 2010. Right insula for our sense of limb ownership and self-awareness of actions. Brain Struct. Funct. 214, 411–417. https://doi.org/10.1007/s00429-010-0250-4.
Kingma, B., Frijns, A., van Marken Lichtenbelt, W., 2012. The thermoneutral zone: implications for metabolic studies. Front. Biosci. (Elite Ed.) 4, 1975–1985. https://doi.org/10.2741/518.
Kucyi, A., Moayedi, M., Weissman-Fogel, I., Hodaie, M., Davis, K.D., 2012. Hemispheric asymmetry in white matter connectivity of the temporoparietal junction with the insula and prefrontal cortex. PLoS One 7, e35589. https://doi.org/10.1371/journal.pone.0035589.
Kuno, S., 1987. A two-dimensional model expressing thermal sensation in transitional conditions. ASHRAE Trans. 93, 396–406.
Kurth, F., Zilles, K., Fox, P.T., Laird, A.R., Eickhoff, S.B., 2010. A link between the systems: functional differentiation and integration within the human insula revealed by meta-analysis. Brain Struct. Funct. 214, 519–534. https://doi.org/10.1007/s00429-010-0255-z.
Menon, V., Uddin, L.Q., 2010. Saliency, switching, attention and control: a network model of insula function. Brain Struct. Funct. 214, 655–667. https://doi.org/10.1007/s00429-010-0262-0.
Moeller, S., Yacoub, E., Olman, C.A., Auerbach, E., Strupp, J., Harel, N., Uğurbil, K., 2010. Multiband multislice GE-EPI at 7 tesla, with 16-fold acceleration using partial parallel imaging with application to high spatial and temporal whole-brain fMRI. Magn. Reson. Med. 63, 1144–1153. https://doi.org/10.1002/mrm.22361.
Mower, G.D., 1976. Perceived intensity of peripheral thermal stimuli is independent of internal body temperature. J. Comp. Physiol. Psychol. 90, 1152–1155. https://doi.org/10.1037/h0077284.
Nakamura, M., Yoda, T., Crawshaw, L.I., Kasuga, M., Uchida, Y., Tokizawa, K., Nagashima, K., Kanosue, K., 2013. Relative importance of different surface regions for thermal comfort in humans. Eur. J. Appl. Physiol. 113, 63–76. https://doi.org/10.1007/s00421-012-2406-9.
Nakamura, M., Yoda, T., Crawshaw, L.I., Yasuhara, S., Saito, Y., Kasuga, M., Nagashima, K., Kanosue, K., 2008. Regional differences in temperature sensation and thermal comfort in humans. J. Appl. Physiol. (1985) 105, 1897–1906. https://doi.org/10.1152/japplphysiol.90466.2008.
Oi, H., Hashimoto, T., Nozawa, T., Kanno, A., Kawata, N., Hirano, K., Yamamoto, Y., Sugiura, M., Kawashima, R., 2017. Neural correlates of ambient thermal sensation: an fMRI study. Sci. Rep. 7, 11279 https://dx.doi.org/10.1038%2Fs41598-017-11802-z.
Olausson, H., Charron, J., Marchand, S., Villemure, C., Strigo, I.A., Bushnell, M.C., 2005. Feelings of warmth correlate with neural activity in right anterior insular cortex. Neurosci. Lett. 389, 1–5. https://doi.org/10.1016/j.neulet.2005.06.065.
Peltz, E., Seifert, F., DeCol, R., Dörfler, A., Schwab, S., Maihöfner, C., 2011. Functional connectivity of the human insular cortex during noxious and innocuous thermal stimulation. Neuroimage 54, 1324–1335. https://doi.org/10.1016/j.neuroimage.2010.09.012.
Ptak, R., 2012. The frontoparietal attention network of the human brain: action, saliency, and a priority map of the environment. Neuroscientist 18, 502–515. https://doi.org/10.1177/1073858411409051.
Rolls, E.T., Grabenhorst, F., Parris, B.A., 2008. Warm pleasant feelings in the brain. Neuroimage 41, 1504–1513. https://doi.org/10.1016/j.neuroimage.2008.03.005.
Schlereth, T., Baumgärtner, U., Magerl, W., Stoeter, P., Treede, R.D., 2003. Left-hemisphere dominance in early nociceptive processing in the human parasylvian cortex. Neuroimage 20, 441–454. https://doi.org/10.1016/s1053-8119(03)00345-8.
Slotnick, S.D., 2017. Cluster success: fMRI inferences for spatial extent have acceptable false-positive rates. Cogn. Neurosci. 8, 150–155. https://doi.org/10.1080/17588928.2017.1319350.
Symonds, L.L., Gordon, N.S., Bixby, J.C., Mande, M.M., 2006. Right-lateralized pain processing in the human cortex: an FMRI study. J. Neurophysiol. 95, 3823–3830. https://doi.org/10.1152/jn.01162.2005.
Talairach, J., Tournoux, P., 1988. Co-Planar Stereotaxic Atlas of the Human Brain, Thieme Verlag, New York.
Thiebaut de Schotten, M., Dell'Acqua, F., Forkel, S.J., Simmons, A., Vergani, F., Murphy, D.G., Catani, M., 2011. A lateralized brain network for visuospatial attention. Nat. Neurosci. 14, 1245–1246. https://doi.org/10.1038/nn.2905.
Tseng, M.T., Tseng, W.Y., Chao, C.C., Lin, H.E., Hsieh, S.T., 2010. Distinct and shared cerebral activations in processing innocuous versus noxious contact heat revealed by functional magnetic resonance imaging. Hum. Brain Mapp. 31, 743–757. https://doi.org/10.1002/hbm.20902.
Youell, P.D., Wise, R.G., Bentley, D.E., Dickinson, M.R., King, T.A., Tracey, I., Jones, A. K., 2004. Lateralisation of nociceptive processing in the human brain: a functional magnetic resonance imaging study. Neuroimage 23, 1068–1077. https://doi.org/10.1016/j.neuroimage.2004.07.004.